CD38-driven mitochondrial trafficking promotes bioenergetic plasticity in multiple myeloma

Christopher R. Marlein[1], Rachel E. Piddock[1], Jayna J. Mistry[1], Lyubov Zaitseva[1], Charlotte Hellmich[1,2], Rebecca H. Horton[1], Zhigang Zhou[1], Martin J. Auger[2], *Kristian M. Bowles[1,2], *Stuart A. Rushworth[1]

[1]Norwich Medical School, The University of East Anglia, Norwich Research Park, NR4 7TJ, United Kingdom
[2]Department of Haematology, Norfolk and Norwich University Hospitals NHS Trust, Colney Lane, Norwich, NR4 7UY, United Kingdom

* denotes joint corresponding authors

Running title

Myeloma uses OXPHOS after mitochondrial transfer

Corresponding Authors

Stuart Rushworth and Kristian Bowles,' Norwich Medical School, The University of East Anglia, Norwich Research Park, NR4 7TJ, United Kingdom, Email: s.rushworth@uea.ac.uk or k.bowles@uea.ac.uk.

Conflict of interest

The authors declare no potential conflicts of interest

Abstract

Metabolic adjustments are necessary for the initiation, proliferation, and spread of cancer cells. Although mitochondria have been shown to move to cancer cells from their microenvironment, the metabolic consequences of this phenomenon have yet to be fully elucidated. Here we report that multiple myeloma (MM) cells use mitochondrial-based metabolism as well as glycolysis when located within the bone marrow microenvironment (BMM). The reliance of MM cells on oxidative phosphorylation was caused by intercellular mitochondrial transfer to MM cells from neighboring non-malignant bone marrow stromal cells (BMSC). This mitochondrial transfer occurred through tumor-derived tunneling nanotubes (TNT). Moreover, shRNA mediated knockdown of CD38 inhibits mitochondrial transfer and TNT formation in-vitro and blocks mitochondrial transfer and improves animal survival in vivo. This study describes a potential treatment strategy to inhibit mitochondrial transfer for clinical benefit and scientifically expands the understanding of the functional effects of mitochondrial transfer on tumor metabolism.

Statement of Significance

Multiple myeloma relies on both oxidative phosphorylation and glycolysis following acquisition of mitochondria from its bone marrow microenvironment.

Introduction

The process by which a rapidly proliferating cancer cell fuels its metabolic requirements is a highly attractive therapeutic target. Warburg stated in 1956 that malignant cells generally use the non-mitochondrial based method of glycolysis to generate its ATP requirements (1). Multiple myeloma (MM) is a hematologic malignancy characterised by the accumulation of monoclonal plasma cells within the bone marrow (2) and is reported to be reliant on glycolysis due to its susceptibility to glycolysis inhibitors such as dichloroacetate (DCA) (3), as well as an elevated glycolytic gene profile (4). However, MM cells do have the capability of using mitochondrial based oxidative phosphorylation under ritonavir treatment (5) and HIF-1α suppression (6).

Oxidative phosphorylation generates a larger quantity of ATP than glycolysis, and occurs within the mitochondria of eukaryotic cells (7). This organelle was originally thought to reside in its somatic cell for its life, however the Gerdes laboratory showed that mitochondria can move between cells (8). This phenomenon has now been reported in models of human cancer including lung (9), bladder (10), breast (11) and melanoma (12,13). Mitochondrial transfer has also recently been shown patho-physiologically, not using models, in canine transmissible cancer (14). Bone marrow stromal cells, which reside in the MM microenvironment, have been shown to be donors in malignant mitochondrial transfer to acute myeloid leukemia blasts (15,16) and non-malignant transfer to lung epithelial cells (17). Others have shown non-malignant transfer of mitochondrial from astrocytes to neurons after stroke is controlled by CD38 (18). These studies indicate that the trafficking of mitochondrial between cells has a role in adapting metabolic processes in both non-malignant and malignant cells.

MM is currently incurable with only half of patients surviving beyond 5 years post diagnosis (19). MM is a tumor highly dependent on the bone marrow microenvironment (BMM) which functions in a supportive role to promote tumor proliferation, survival and migration (20). Preclinical studies of CD38 inhibition in myeloma shows that it mediates MM cytotoxicity in the presence of the protective bone marrow niche (21) and in early phase clinical studies anti-CD38 directed

therapy showed clinical benefit as a single agent in myeloma patients (22,23). Furthermore, phase 3 clinical trials in MM patients of anti-CD38 antibody therapy given in addition to chemotherapy, have demonstrated improvements in overall response rates and progression free survival (24,25) and lower risk of death (26) in patients receiving the antibody with chemotherapy compared to chemotherapy alone. Daratumumab has now been FDA approved for the treatment of relapse refractory myeloma in combination with bortezomib or lenalidomide (27).

In this study, we look to determine first if the MM microenvironment supports MM proliferation, by promoting mitochondrial based oxidative phosphorylation. Second, we analyse whether the transfer of mitochondria to malignant plasma cells, from BMSC, regulates the metabolic process. Next, we aim to dissect the mechanisms which facilitate the interaction allowing the BMSC to transfer mitochondria to MM. Finally, we aim provide a novel therapeutic paradigm for the targeting of mitochondrial transfer as an anti-cancer therapy.

Methods

Primary cell culture

Patient bone marrow was obtained following informed written consent and under approval by the Health Research Authority of the National Health Service, United Kingdom (LRECref07/H0310/146) and in accordance with the Declaration of Helsinki. All patient details are provided in table 1. Primary MM cells were isolated by histopaque density centrifugation and purified by positive selection using magnetic-activated cell sorting with CD138+ microbeads (Miltenyi Biotec), cell type was confirmed by flow cytometry as previously described (28). Bone marrow stromal cells (BMSC) were isolated from MM patient samples by adherence to tissue culture plastic and were then expanded in Dulbecco's modified Eagle's Medium (DMEM) containing 10% foetal bovine serum (FBS) and supplemented with 1% penicillin-streptomycin (Hyclone, Life Sciences) (29). BMSC markers were confirmed using flow cytometry for expression of CD90+, CD73+, CD105+ and CD45-. BMSCs were passaged three times before use in the assays presented in this manuscript (30).

Human Cell lines

The MM-derived cell lines were obtained from the European Collection of Cell Cultures (ECACC) where they are authenticated by DNA fingerprinting. The cells were periodically tested for mycoplasma contamination, using the MycoProbe, Mycoplasma Detection Kit purchased from R&D systems (Minneapolis, MN) in Jan 2018. These cells were cultured in Roswell Park Memorial Institute (RPMI) 1640 medium supplemented with 10% foetal bovine serum, 1% penicillin-streptomycin (Hyclone, Life Sciences). All cell lines were used between passage 4-15 from the time of purchase.

MitoTracker based mitochondrial transfer assay

To assess and quantify mitochondrial transfer from BMSC to MM cells the MitoTracker based staining assay developed in our laboratory was used (15). Briefly, human primary BMSC were stained with 200 nM MitoTracker Green FM for 1 hour. Primary and cell line MM were also stained with 200 nM MitoTracker Green FM for 30 minutes, to eliminate dye leakage. Both cell types were washed three times in phosphate buffered saline (PBS) to remove the unbound probe. Stained MM cells were added to stained BMSC at a 5:1 ratio for 24 hours. Stained MM cells were also

grown in mono-culture for 24 hours as a control. After incubation MM cells were removed from BMSC and MitoTracker fluorescence in these cells was analysed using the CyFlow Cube 6 flow cytometer (Sysmex, Milton Keynes). For mitochondrial quantification, the difference in MitoTracker fluorescence between MM cells grown with and without BMSC provided a baseline mitochondrial transfer. The effect of Cytochalsin B (350 μM), Dansylcadavarine (50 μM), Bortezomib (10 nM), CD38-blocking antibody or CD38 knockdown (KD) MM cells on mitochondrial transfer was achieved using this method.

rLV.EF1.mCherry mitochondrial transfer assay

rLV.EF1.mCherry lentivirus was purchased from Clontech Takara Bio Europe (Saint-Germain-en-Laye, France). Primary human BMSC were transduced with this virus for 72 hours and cultured for 1 week before use, to ensure no residual lentivirus remained. RPMI cells were cultured with rLV.EF1.mCherry BMSC for 1 week, and imaged using the Zeiss LSM 800 Axio Observer.Z1 confocal microscope with a 40X water objective (Carl Zeiss).

MM xenograft model

For this study the NOD.Cg-Prkdcscid IL2rgtm1Wjl/SzJ (NSG) mice (The Jackson Laboratory, Bar Harbour, ME, USA RRID:IMSR_NM-NSG-001). were housed under specific pathogen-free conditions in a 12/12-hour light/dark cycle with food and water provided *ad libitum* in accordance with the Animal Scientific Procedures Act, 1986 (UK) and under UK Home Office and Institutional Animal Welfare and Ethics Review board approvals. $0.5x10^6$ MM1S or U266 MM cell lines were intravenously injected into non-irradiated 6-8 week old NSG mice for mouse mtDNA detection. $1.0x10^6$ MM1S-luc cells were injected for the *ex vivo* Seahorse extracellular flux assay. $0.5x10^6$ MM1S-luc cells were injected for the CD38 KD xenograft. Mice injected with MM1S-luc cells were monitored via in-vivo bioluminescent imaging (Bruker, Coventry UK), as previously described (31). At pre-defined humane end points mice were sacrificed (6-12 weeks post injection), bone marrow isolated and engraftment determined. Human MM cells were purified from the heterogeneous bone marrow by MACS microbeads. This purified human MM cell population was used for the PCR

and agarose gel electrophoresis. Levels of mitochondria in the purified MM1S-luc populations was achieved using MitoTracker Green FM staining and flow cytometry.

Seahorse extracellular flux assay

Oxidative phosphorylation and glycolysis rates were assessed in MM cells using the Seahorse XFp Analyzer, as previously described (29) and the Seahorse XF Mito stress test kit (Agilent Seahorse Bioscience), according to manufacturer's specifications. Co-cultures of primary human BMSC and MM cells were prepared in a 1:5 ratio for 24 hours. Further information can be found in supplementary methods section.

Murine mitochondrial DNA detection

Murine mitochondrial DNA (mtDNA) detection was used to determine if inter-species mitochondrial transfer occurred from murine BMSC to human MM cells, as previously described (15). DNA from the purified human MM cells were extracted using the GenElute mammalian DNA miniprep kit. 8 ng of DNA was added to the PCR reaction containing Sybr green and murine primers provided in the Detroit R&D kit. PCRs were amplified for 40 cycles (95°C/15 seconds, 60°C/60 seconds) on a Roche 96-well LightCycler480. PCR products were run on a 1.25% agarose gel at 100V for 1 hour. Detection was performed by Chemdoc-It2 Imager (UVP) and analysed using ImageJ. We were able to quantify movement of mitochondria between murine bone marrow cells and human MM cells using species specific Taqman probes purchased from ThermoFisher (Waltham, MA, USA). These contained murine and human ND1 mitochondrial probes (on VIC and FAM fluorophores) along with murine and human TERT genomic probes. Extracted DNA was amplified for 40 cycles (95°C/15 seconds, 60°C/60 seconds) on a Roche 96-well LightCycler480. mtDNA copy numbers were determined for both human and murine mitochondria using the $\Delta\Delta$Ct method, using human genomic TERT to normalise results. These values were used to generate the percentage of mouse mitochondria in the human MM cells, ultimately used to quantify mitochondrial transfer.

Confocal Microscopy

To visualise TNTs BMSC were stained with 200 nM MitoTracker green FM and MM cells were stained with Vybrant Dil stain to visualise cell membranes. After co-culture cells were fixed with 4% paraformaldehyde and imaged. In addition, the rLV.EF1.AcGFP-Mem9 lentivirus was purchased from Clontech Takara Bio Europe (Saint-Germain-en-Laye, France), enabling the stable tagging of plasma membranes with a GFP fluorophore. MM1S cells were transduced with this lentivirus and cultured for 72 hours prior to use. BMSC were stained with 200nM MitoTracker CMXRos and cultured with MM1S cells transduced as above for 24 hours, before fixation with paraformaldehyde. Confocal images were acquired on Zeiss LSM 800 Axio Observer.Z1 confocal microscope with a 40X water objective (Carl Zeiss) and a Zeiss AxioPlan 2ie (Carl Zeiss). The frequency of TNT formation was analysed through quantifying TNT anchor points (TAPs), on BMSC after co-culture with MM cells, per confocal image as previously described (15). TAPs were also assessed under Cytochalasin B treatment and with CD38 KD MM cell lines.

Results

MM metabolic plasticity

To determine the role of the bone marrow microenvironment on metabolism of malignant plasma cells we analysed the metabolic output (OCR and ECAR) of primary MM cells, at point of isolation from the human bone marrow and compared this to MM cell lines grown in culture. Figures 1A and B show that primary MM cells (n=4) have increased mitochondrial based metabolism compared to cell lines (n=4). The levels of glycolysis, measured by extracellular acidification, is lower in primary MM compared to MM cell lines (Figure 1C). To further investigate this difference in-vivo we compared the OCR and lactate levels in MM1S cells cultured in-vitro to MM1S cells post engraftment in NSG mice. We found increased mitochondrial based metabolism in the MM1S isolated from the mouse compared to the cells grown in-vitro (Figures 1D and E), with no difference observed in glycolysis levels (Figure 1F). Next, we compared the bioenergetics of MM cell lines grown alone or with primary bone marrow stromal cells (BMSC). Increased mitochondrial metabolism was observed in cell lines cultured with BMSC compared to cell lines cultured alone (Figure 1G, H, I). Finally, we show that MM cell lines have increased ATP production and proliferation when cultured with BMSC (Figure 1J).

To determine whether the increase in mitochondrial metabolism is due to the direct contact between BMSC and MM cells, we repeated the Seahorse extracellular flux assay with MM cells cultured for 24 hours in BMSC conditioned medium +/- 0.2µM filtration. The increased mitochondrial metabolism and increase in ATP production is not observed in MM cultured in BMSC conditioned medium (Figure 1K and L); highlighting the need for direct contact between BMSC and MM cells for the bio-energetic effect observed. To further examine this process, we treated BMSC with 25µM Rotenone to inhibit BMSC mitochondria. Figure 1M presents that MM cells cultured on Rotenone treated BMSC have lower levels of mitochondrial respiration. Furthermore, the addition of dimethyl succinate directly to MM cells (without BMSC) had no effect on OCR (Figure S1A). This shows that the mitochondrial metabolic

status of BMSC plays a role in the bio-energetic flexibility in MM cells after culture with BMSC. Furthermore, we isolated mitochondria from BMSC and MM cells and analysed the levels of OCR. We found BMSC mitochondria to have a 10-fold increase in OCR compared to MM cells, highlighting that BMSC mitochondria are more functional (Figure S1B). Finally, we examined the effect of 10mM glucose, compared to 2.5mM, on mitochondrial respiration in MM cells. Figure 1N shows that the same increase in mitochondrial respiration is observed between the two glucose conditions.

Mitochondria are transferred from BMSC to Multiple Myeloma cells

To understand how MM can switch on oxidative phosphorylation when in the presence of BMSC we explored the possible transfer of mitochondria from BMSC to MM. The transfer of mitochondria from non-malignant cells of the tumor microenvironment to malignant cells has recently been reported in a number of cancers including acute myeloid leukemia and melanoma (9,11,12,15,16). To determine if MM acquire mitochondria from BMSC to support oxidative phosphorylation, we employed three methods. First, we used a MitoTracker mitochondrial transfer assay (15); where both BMSC and MM cells are stained with MitoTracker and cultured together and any increases in MitoTracker fluorescence after co-culture in tumor cells shows mitochondrial transfer has occurred. Primary MM samples (n=10) cultured on BMSC have increased MitoTracker levels compared to mono-cultured MM cells (Figure 2A). This is also the case for 4/5 MM cell lines tested; MM1S, U266, RPMI and H929, shown in Figure 2B. Second, we infected primary BMSC with an rLV.EF1.mCherry lentivirus for stable production of mitochondria-incorporated mCherry tagged protein. Figure 2C shows upon the culture of MM cell lines on these infected BMSC, the MM acquire the mCherry fluorescence.

Finally, we used an in-vivo model to determine if mitochondrial transfer occurs within the malignant BM. To do this MM1S and U266 MM cell lines were engrafted into NSG mice, following tumor engraftment we isolated the human MM cells and determined if mouse mtDNA could be detected in human MM cells after extraction from mouse BM. We transplanted 3 animals with MM1S and 3 with U266 MM cells, all animals engrafted with the MM cell line (Figure S2A). Human MM cells were

sorted from mouse bone marrow cells, achieving a 98.53% human population (Figure S2B). We extracted DNA from the purified MM population and performed a PCR analysing mouse mitochondrial DNA and mouse genomic DNA. Figure 2D shows that MM cells isolated from engrafted NSG mice contained mouse mitochondrial DNA but not mouse genomic DNA.

To determine whether the mitochondria that enter the malignant plasma cells are functional, we treated MM cell lines and primary MM cells (n=5) with rotenone to inhibit mitochondrial function and assess whether function can be restored by co-culture with BMSC. Figure 2E shows that primary MM have reduced TMRM fluorescence when treated with rotenone but this is prevented when cultured on BMSC. Figure 2F shows that TMRM fluorescence is higher in rotenone treated MM that have been cultured with BMSC compared to mono-culture. Since oxidative stress increases mitochondrial transfer from non-malignant cells to malignant cells (15) and chemotherapy treatment induces oxidative stress, we wanted to determine if the MM chemotherapy drug, bortezomib, increased mitochondrial transfer. We found that the addition of bortezomib to the co-culture, between BMSC and primary MM cells (n=7), increased mitochondrial transfer (Figure 2G). This was also the case in four MM cell lines, where mitochondrial transfer was increased (Figure 2H).

Additionally, we quantified the levels of transfer in-vitro using qPCR with species specific Taqman probes. We cultured human MM cell lines with the murine BMSC cell line M2-10B4 for 24 hours, extracted DNA and carried out a qPCR with probes designed to detect human and murine ND1. We found 3% of the total mitochondria in the human MM cell to be of mouse origin (Figure S3A). Finally, to demonstrate that the 3% of transferred mitochondria are having significant effects on MM cell OXPHOS we generated rho0 BMSC (Figure S3B) and cultured MM cells on both rho0 BMSC and control BMSC. Figure 2I shows that MM cells cultured on rho0 BMSC have lower levels of mitochondrial respiration (basal and maximal) compared to MM cells cultured on control BMSC.

Mitochondrial transfer in Multiple Myeloma is via TNTs

Mitochondria have been reported to move via both TNTs (10,15,32) and endocytosis (16). To understand how mitochondria move to MM we used TNT and endocytosis

inhibitors, Cytochalasin B and Dansylcadavarine respectively. Cytochalasin B reduced mitochondrial transfer to MM cell lines by up to 46.19% (Figure 3A), whereas there was no significant reduction observed with Dansylcadavarine (Figure 3B). We also found no mitochondrial transfer occurred from BMSC to malignant plasma cells when MM were cultured in a transwell system (Figure S4). Next, we used fixed cell confocal microscopy to visualise the highly dynamic TNTs. To do this we stained MM cells with the Vybrant lipid stain (red) and the mitochondria in BMSC with MitoTracker Green stain and then cultured the cells together for 24 hours. Following co-culture, the cells were fixed and TNT formation was detected using confocal microscopy. We observed red TNTs formed between BMSC and the MM cell line MM1S (Figure 3C) and green mitochondria from the BMSC located in the MM1S cells. Additionally, we stably expressed GFP in the plasma membrane of MM cells, using a lentivirus, and cultured them with MitoTracker Red CMXRos. We visualised green TNTs between MM cells and BMSC, using fixed cell confocal microscopy, with red mitochondria within the nanotube (Figure 3D and E). Using this method, we found approximately 60% of the MM cells had visible TNT projections (Figure S5A).

To quantify the number of TNTs formed during a co-culture we used TNT anchor points (TAPs) and confocal microscopy, as previously described (15). TAPs are residual plasma cell derived Vybrant DiI stain which remains on BMSC after TNT contact. TAPs can be observed in co-cultures of MM cells and BMSC (Figure 3F). We show that TAPs can also be visualised between GFP plasma membrane tagged MM cells and MitoTracker CMXRos stained BMSC (Figure S5B and C). Quantification of TAPs in four MM cell lines, shows a median of 232.5 (range, 218-278) - TAPs per confocal image (Figure S6). Upon Cytochalasin B treatment, the number of TAPs was significantly reduced (median reduction: 75.09%, range: 71.3-79.27%) (Figure 3G). No TAPs are formed when MM cells are cultured in a transwell system or when medium from Vybrant DiI stained MM cells is added to BMSC, therefore confirming that TAPs are only present when the two cell types are in direct contact (Figure S7).

CD38 inhibition prevents mitochondrial transfer and TNT formation

Hayakawa and colleagues recently reported that mitochondria are released by astrocytes as mitochondria-containing particles, in a CD38-dependent process, and recaptured by neurons (18). Studies have shown that CD38 expression in MM is high compared to non-malignant plasma cells (33). Therefore, we correlated the CD38 expression levels to mitochondrial transfer levels of the MM cell lines and primary MM cells (n=12). We found there to be a strong correlation (R=0.7915; P=0.0013) (Figure 4A). Using a CD38 blocking antibody, mitochondrial transfer to primary MM is significantly reduced (n=8) (Figure 4B). Knockdown of CD38 in the MM cell lines; MM1S, U266, RPMI and H929 (Figure 4C and Figure S8) reduced mitochondrial transfer from BMSC to MM (Figure 4D). We next analysed the cell viability and levels of apoptosis in CD38 KD and control KD cells cultured with BMSC. We found there to be decreased cell viability and increased levels of apoptosis in CD38 KD cells compared to control KD cells (Figure 4E and F).

A recent study identified that all-trans retinoic acid (ATRA) increases CD38 expression on AML (34). We next identified if this was the case for MM. Figure 4G and H show CD38 is upregulated in MM cells after 1 μM ATRA treatment both at RNA and protein levels. We tested whether this increase in CD38 induces mitochondrial transfer, Figure 4I shows that this is the case with increased levels of mitochondrial transfer found in three MM cells lines tested. Taken together these results show functionally that mitochondrial transfer from BMSC to MM cells requires CD38 and supports multiple myeloma growth and survival.

Tumor cell CD38 supports the formation of TNTs

CD38 is known to facilitate the adhesion of leukocytes to endothelial cells (35), therefore we hypothesised that CD38 has a role in the formation of the TNT. TAP quantification was used in co-cultures between BMSC and control KD or CD38 KD MM cell lines. Figure 5A shows reduced TAP formation by U266 and RPMI in CD38 KD cells. This result is replicated with MM1S and H929 MM cell lines, Figure 5B. Observations show that TAP formation leaves some residual MM cell membrane on the BMSC. To determine if MM derived CD38 is part of this residual membrane that is left on the BMSC after TAP formation flow cytometry was used to detect CD38 expression on MM and BMSC before and after co-culture. Figure 5C shows that CD38 expression is lower on MM after co-culture with BMSC, whereas CD38 can be

detected on BMSC after MM co-culture (Figure 5D). Figure 5E shows that CD38 localises to TAPs on BMSC after co-culture with MM.

Targeting CD38 in-vivo blocks mitochondrial transfer and improves animal survival

To determine the in-vivo significance of CD38 inhibition on mitochondrial transfer we engrafted control KD and CD38 KD MM1S-luc cells into NSG mice. MM disease progression in these mice was analysed weekly by live animal bioluminescence, which revealed that there was consistently reduced tumor burden in the bone marrow with CD38 KD cells (Figure 6A). Survival of mice transplanted with CD38 KD cells had a significantly increased survival time compared to control KD cells (Figure 6B) but no difference in the growth capability when cultured in-vitro (figure 6C). Analysis of the BM confirmed engrafted into NSG mice (Figure S9).

To determine if mitochondrial transfer was affected by CD38 KD we assessed the levels of mitochondria post-engraftment in the human MM cell population, using MitoTracker Green staining. MM cells post-engraftment, have significantly reduced mitochondrial levels in CD38 KD cells compared to control KD cells, however no difference was observed when cultured in-vitro (Figure 6D and 6E). Finally, we measured the mitochondrial respiration rates in CD38 KD MM1S cells grown in-vitro with and without BMSC. Figure 6F and 6G shows that there is significant reduction in mitochondrial respiration in CD38 KD cells grown with BMSC compared to control KD cells. No difference in mitochondrial respiration was observed between CD38 KD and control KD cells grown without BMSC. These results identify in-vivo, a functional, pro-tumoral role for CD38-driven mitochondrial transfer in MM.

Discussion

The biologic phenomenon of mitochondrial trafficking between non-malignant cells and malignant cells is increasingly becoming recognised as part of the cancer phenotype. This process provides the oxidative phosphorylation machinery to enable increased ATP production to aid cancer progression. Here we examine the metabolic changes resultant from mitochondrial transfer in multiple myeloma which to date has been regarded as a glycolytic tumor (3-5).

In this study, we investigate the influence of the BM on the energy output of MM. MM cells are known to generally use the non-mitochondrial based process of glycolysis to generate its ATP and have been shown to be susceptible to glycolysis inhibitors (3,5), these studies have only focussed on MM cell lines not in the presence of their protective microenvironment. The study by Dalva-Aydemir and colleagues show that MM cell lines have the capability of undergoing functional oxidative phosphorylation after treatment with the glycolysis inhibitor ritonavir (5). Further data proposing a reliance on glycolysis in MM was provided by a Fujiwara et al (2013) who showed increased expression of genes associated with a glycolytic profile in primary MM. Moreover, others have shown that PET imaging can be used in the diagnosis of myeloma and results show that high glucose uptake is associated with poor prognosis (36,37). In our study, we show that MM within the BMM utilise oxidative phosphorylation and glycolysis to provide the necessary energy for survival and proliferation. Interestingly, others have shown that that glucose can feed the TCA cycle via circulating lactate derived from glycolysis (38). Moreover, the authors of this manuscript show that lactate (derived from glycolysis) is a primary TCA substrate in lung tumours. Another study shows that lactate can feed the TCA cycle in both human and mouse tumours (39). Therefore, we hypothesise based on these reports and data from our own experiments that in myeloma (and potentially other tumors) glucose is used by glycolysis (PET scan positive); the metabolite, lactate, is then fed into the TCA cycle to generate ATP by oxidative phosphorylation in presence of functional mitochondria, which have been derived from the bone marrow stromal cells.

We demonstrate that mitochondrial trafficking from BMSC to MM orchestrates this plasticity in MM metabolism. Cytochalasin B (which inhibits TNT formation) reduced

mitochondrial transfer to MM cell lines by approximately one half, establishing mechanistically that MM can be added to an emerging list of tumors which are capable of acquiring mitochondria from neighbouring non-malignant cells through TNTs (11,15,22,32). Furthermore, transferred mitochondria were found to metabolically promote oxidative phosphorylation, which was functionally beneficial to the tumor and remained so in the presence of chemotherapy treatment. Pro-tumoral mitochondrial transfer therefore can be considered part of the malignant phenotype of the disease and in addition contributes to the cancer cell survival response to chemotherapy. As the number of tumors in which this phenomenon is identified grows, it becomes increasingly likely that mitochondrial transfer through TNTs forms, more broadly, a fundamental component of a common malignant phenotype.

CD38 has a dual role as both a receptor involved in the migration of leukocytes (40) and as an ectoenzyme catalysing the formation of ADPR from NAD+ (41). Originally thought to be expressed only on hematopoietic and neuronal cells, CD38 is now known to be expressed on many other cell types such as prostate (42), lung (43) and skin cells (44). CD38 has recently been shown to have a role in the movement of mitochondria between astrocytes to damaged neurons post stroke (18). In this study mitochondria were shown to move in micro-vesicles which enabled the restoration of metabolic potential and survival of neurons after stroke, this process was shown to be dependent on CD38. Others have shown that LPS induces mitochondrial transfer from BMSC to alveoli (17) and LPS can induce CD38 upregulation (45). We further present that mitochondrial transfer in MM is via a CD38-dependant mechanism, independent of micro-vesicle transfer. CD38 inhibition reduced TAP formation in our study directly linking MM nanotube attachment to non-malignant stromal cells and tumor CD38 expression. Metabolically we observed a significant reduction in mitochondrial respiration in CD38 KD MM cells grown with BMSC compared to control KD cells (and this was only seen when cells were co-cultured with stromal cells rather than monoculture). Functionally in-vivo CD38 KD improved animal survival and tumor cells from CD38 KD MM contained significantly fewer mitochondria. These data establish that mitochondrial transfer in MM is biologically and metabolically relevant and furthermore leads us to hypothesise that similar CD38 driven mitochondrial transfer may be relevant in other malignancies. Presently it remains unexplained whether mitochondrial transfer occurs through CD38 activity

as a cell surface receptor or ectoenzyme or through a hitherto unknown function of CD38.

Drugs targeting CD38 have recently been shown to be well tolerated and clinically efficacious in early phase studies of the treatment of relapsed refractory MM (23). Pre-clinical studies found that the anti-CD38 antibody daratumumab mediates MM cytotoxicity in the presence of the protective bone marrow, via immune mediated killing, either antibody-dependent cell-mediated cytotoxicity (ADCC) or complement-dependent cytotoxicity (CDC) (21,22). As daratumumab also downregulates CD38+ regulatory T and B cells, a combination with immunomodulatory drugs has been postulated to be advantageous. The use of daratumumab containing treatment combinations has shown significant clinical benefit in patients with both previously untreated and relapsed MM (24-26). Although we have not tested daratumumab in this study, our results provide an alternative mechanism of action of drugs targeting CD38, showing that inhibiting CD38 can reduce mitochondrial transfer. Inhibition of mitochondrial transfer also significantly reduces the mitochondrial oxidative metabolism in the MM cell when cultured with BMSC. We show in mouse models that MM disease progression is reduced when CD38 is knocked down in MM cells, we assign this phenotype in part to reduced mitochondrial transfer levels. Moreover, to overcome MM relapse following the use of chemotherapy agents such as bortezomib, we propose the testing of combinations of drugs targeting CD38 with established chemotherapy agents including cytotoxics and proteasome inhibitors. If anthracyclines and proteasome inhibitors are known to induce mitochondrial transfer then conceptually anti-CD38 therapy may work well as an adjunct in multi-agent combinations.

For mitochondrial transfer to be targeted therapeutically in the clinic, viable molecular targets involved in the transfer process need to be elucidated. We recently identified that NOX2 derived superoxide from AML, is crucial for mitochondrial transfer to occur in this malignancy (15). However, inhibitors of NOX2 are not clinically available and moreover toxicity may be present a problem with such a strategy as deletion of NOX2 in humans frequently leads to death in the first decade of life (46). Here our results identify CD38 as a viable molecular target to reduce mitochondrial transfer between non-malignant and malignant cells, with drugs presently available for use

and/or in advanced stages of pre-clinical development. With CD38 expression now known on a wide variety of malignant cells (47), our data leads us to hypothesise that CD38 has a potential clinical role in other cancers with mitochondrial transfer systems. Furthermore, we should look to identify alternate functional receptors in non-CD38 expressing tumors, with possible candidates including CD157, the only other known member of the CD38 superfamily.

In this study, we present a paradigm to target mitochondrial transfer as a means to perturb tumor metabolism and function as an anti-cancer therapeutic strategy. Here we show that CD38 is required for the formation of TNTs facilitating pro-tumoral mitochondrial transfer in MM. We show increased levels of apoptosis are observed in malignant plasma cells when the number of mitochondria transferred is reduced demonstrating this process is pro-tumoral in MM. Moreover, BMSC derived mitochondria are more functional than MM derived mitochondria, therefore it is metabolically advantageous to the MM cell to acquire the BMSC mitochondria. Alternate mechanisms exist to enhance tumoral metabolic activity such as acquisition of extracellular metabolites (48). However, this does not appear to be a significant factor in MM as in our experiments mitochondrial respiration remained constant when metabolite containing BMSC medium was added to MM indirectly and when dimethyl succinate was added to MM cells independently of BMSC.

Overall the trafficking of mitochondria allows MM cells to switch on mitochondrial oxidative metabolism to increase ATP production. Through CD38 inhibition, mitochondrial transfer is reduced in-vitro and in-vivo and MM disease progression is reduced increasing animal survival. Drugs targeting CD38 are presently being used to treat MM and optimum combinations are being clinically studied. The data presented here explains that CD38 inhibition in MM is therefore a viable treatment strategy to inhibit mitochondrial transfer for clinical benefit. Our study accordingly provides the scientific rationale and metabolic basis for inhibiting mitochondrial transfer in MM, we also provide a biologic rationale for the selection of appropriate drugs to be used in combination with mitochondrial transfer blocking agents and finally we propose the potential of translating these findings to other malignancies and diseases.

Acknowledgements

The authors thank the Rosetrees Trust, The Big C, and the Norwich Research Park Doctoral Training Program for funding. They also thank Professor Richard Ball, Dr Mark Wilkinson, Mr Iain Sheriffs, and Ms Sue Steel, Norwich Biorepository (UK) for help with sample collection and storage. pCDH-luciferase-T2A-mCherry was kindly gifted by Professor Irmela Jeremias, MD, from Helmholtz Zentrum München, Munich, Germany. The authors also thank Allyson Tyler, Ian Thirkettle and Karen Ashurst from the Laboratory Medicine department at the Norfolk and Norwich University Hospital for technical assistance.

References

1. Warburg O. On the origin of cancer cells. Science **1956**;123:309-14
2. Palumbo A, Anderson K. Multiple myeloma. N Engl J Med **2011**;364:1046-60
3. Sanchez WY, McGee SL, Connor T, Mottram B, Wilkinson A, Whitehead JP*, et al.* Dichloroacetate inhibits aerobic glycolysis in multiple myeloma cells and increases sensitivity to bortezomib. Br J Cancer **2013**;108:1624-33
4. Fujiwara S, Kawano Y, Yuki H, Okuno Y, Nosaka K, Mitsuya H*, et al.* PDK1 inhibition is a novel therapeutic target in multiple myeloma. Br J Cancer **2013**;108:170-8
5. Dalva-Aydemir S, Bajpai R, Martinez M, Adekola KU, Kandela I, Wei C*, et al.* Targeting the metabolic plasticity of multiple myeloma with FDA-approved ritonavir and metformin. Clin Cancer Res **2015**;21:1161-71
6. Borsi E, Perrone G, Terragna C, Martello M, Dico AF, Solaini G*, et al.* Hypoxia inducible factor-1 alpha as a therapeutic target in multiple myeloma. Oncotarget **2014**;5:1779-92
7. Gautheron DC. Mitochondrial oxidative phosphorylation and respiratory chain: review. J Inherit Metab Dis **1984**;7 Suppl 1:57-61
8. Rustom A, Saffrich R, Markovic I, Walther P, Gerdes HH. Nanotubular highways for intercellular organelle transport. Science **2004**;303:1007-10
9. Spees JL, Olson SD, Whitney MJ, Prockop DJ. Mitochondrial transfer between cells can rescue aerobic respiration. Proc Natl Acad Sci U S A **2006**;103:1283-8
10. Lu J, Zheng X, Li F, Yu Y, Chen Z, Liu Z*, et al.* Tunneling nanotubes promote intercellular mitochondria transfer followed by increased invasiveness in bladder cancer cells. Oncotarget **2017**;8:15539-52
11. Pasquier J, Guerrouahen BS, Al Thawadi H, Ghiabi P, Maleki M, Abu-Kaoud N*, et al.* Preferential transfer of mitochondria from endothelial to cancer cells through tunneling nanotubes modulates chemoresistance. J Transl Med **2013**;11:94
12. Tan AS, Baty JW, Dong LF, Bezawork-Geleta A, Endaya B, Goodwin J*, et al.* Mitochondrial genome acquisition restores respiratory function and tumorigenic potential of cancer cells without mitochondrial DNA. Cell Metab **2015**;21:81-94
13. Dong LF, Kovarova J, Bajzikova M, Bezawork-Geleta A, Svec D, Endaya B*, et al.* Horizontal transfer of whole mitochondria restores tumorigenic potential in mitochondrial DNA-deficient cancer cells. Elife **2017**;6
14. Strakova A, Ni Leathlobhair M, Wang GD, Yin TT, Airikkala-Otter I, Allen JL*, et al.* Mitochondrial genetic diversity, selection and recombination in a canine transmissible cancer. Elife **2016**;5
15. Marlein CR, Zaitseva L, Piddock RE, Robinson SD, Edwards DR, Shafat MS*, et al.* NADPH oxidase-2 derived superoxide drives mitochondrial transfer from bone marrow stromal cells to leukemic blasts. Blood **2017**;130:1649-60
16. Moschoi R, Imbert V, Nebout M, Chiche J, Mary D, Prebet T*, et al.* Protective mitochondrial transfer from bone marrow stromal cells to acute myeloid leukemic cells during chemotherapy. Blood **2016**;128:253-64
17. Islam MN, Das SR, Emin MT, Wei M, Sun L, Westphalen K*, et al.* Mitochondrial transfer from bone-marrow-derived stromal cells to pulmonary alveoli protects against acute lung injury. Nat Med **2012**;18:759-65

18. Hayakawa K, Esposito E, Wang X, Terasaki Y, Liu Y, Xing C*, et al.* Transfer of mitochondria from astrocytes to neurons after stroke. Nature **2016**;535:551-5
19. Siegel RL, Miller KD, Jemal A. Cancer statistics, 2016. CA Cancer J Clin **2016**;66:7-30
20. Kawano Y, Moschetta M, Manier S, Glavey S, Gorgun GT, Roccaro AM*, et al.* Targeting the bone marrow microenvironment in multiple myeloma. Immunol Rev **2015**;263:160-72
21. de Weers M, Tai YT, van der Veer MS, Bakker JM, Vink T, Jacobs DC*, et al.* Daratumumab, a novel therapeutic human CD38 monoclonal antibody, induces killing of multiple myeloma and other hematological tumors. J Immunol **2011**;186:1840-8
22. Lokhorst HM, Plesner T, Laubach JP, Nahi H, Gimsing P, Hansson M*, et al.* Targeting CD38 with Daratumumab Monotherapy in Multiple Myeloma. N Engl J Med **2015**;373:1207-19
23. Lonial S, Weiss BM, Usmani SZ, Singhal S, Chari A, Bahlis NJ*, et al.* Daratumumab monotherapy in patients with treatment-refractory multiple myeloma (SIRIUS): an open-label, randomised, phase 2 trial. Lancet **2016**;387:1551-60
24. Palumbo A, Chanan-Khan A, Weisel K, Nooka AK, Masszi T, Beksac M*, et al.* Daratumumab, Bortezomib, and Dexamethasone for Multiple Myeloma. N Engl J Med **2016**;375:754-66
25. Dimopoulos MA, Oriol A, Nahi H, San-Miguel J, Bahlis NJ, Usmani SZ*, et al.* Daratumumab, Lenalidomide, and Dexamethasone for Multiple Myeloma. N Engl J Med **2016**;375:1319-31
26. Mateos MV, Dimopoulos MA, Cavo M, Suzuki K, Jakubowiak A, Knop S*, et al.* Daratumumab plus Bortezomib, Melphalan, and Prednisone for Untreated Myeloma. N Engl J Med **2018**;378:518-28
27. Bhatnagar V, Gormley NJ, Luo L, Shen YL, Sridhara R, Subramaniam S*, et al.* FDA Approval Summary: Daratumumab for Treatment of Multiple Myeloma After One Prior Therapy. Oncologist **2017**;22:1347-53
28. Piddock RE, Loughran N, Marlein CR, Robinson SD, Edwards DR, Yu S*, et al.* PI3Kdelta and PI3Kgamma isoforms have distinct functions in regulating pro-tumoural signalling in the multiple myeloma microenvironment. Blood Cancer J **2017**;7:e539
29. Abdul-Aziz AM, Shafat MS, Mehta TK, Di Palma F, Lawes MJ, Rushworth SA*, et al.* MIF-Induced Stromal PKCbeta/IL8 Is Essential in Human Acute Myeloid Leukemia. Cancer Res **2017**;77:303-11
30. Zaitseva L, Murray MY, Shafat MS, Lawes MJ, MacEwan DJ, Bowles KM*, et al.* Ibrutinib inhibits SDF1/CXCR4 mediated migration in AML. Oncotarget **2014**;5:9930-8
31. Vick B, Rothenberg M, Sandhofer N, Carlet M, Finkenzeller C, Krupka C*, et al.* An advanced preclinical mouse model for acute myeloid leukemia using patients' cells of various genetic subgroups and in vivo bioluminescence imaging. PLoS One **2015**;10:e0120925
32. Lou E, Fujisawa S, Morozov A, Barlas A, Romin Y, Dogan Y*, et al.* Tunneling nanotubes provide a unique conduit for intercellular transfer of cellular contents in human malignant pleural mesothelioma. PLoS One **2012**;7:e33093

33. Almeida J, Orfao A, Ocqueteau M, Mateo G, Corral M, Caballero MD*, et al.* High-sensitive immunophenotyping and DNA ploidy studies for the investigation of minimal residual disease in multiple myeloma. Br J Haematol **1999**;107:121-31
34. Buteyn NJ, Fatehchand K, Santhanam R, Fang H, Dettorre GM, Gautam S*, et al.* Anti-leukemic effects of all-trans retinoic acid in combination with Daratumumab in acute myeloid leukemia. Int Immunol **2018**;30:375-83
35. Newman PJ. Switched at birth: a new family for PECAM-1. J Clin Invest **1999**;103:5-9
36. Dammacco F, Rubini G, Ferrari C, Vacca A, Racanelli V. (1)(8)F-FDG PET/CT: a review of diagnostic and prognostic features in multiple myeloma and related disorders. Clin Exp Med **2015**;15:1-18
37. Cavo M, Terpos E, Nanni C, Moreau P, Lentzsch S, Zweegman S*, et al.* Role of (18)F-FDG PET/CT in the diagnosis and management of multiple myeloma and other plasma cell disorders: a consensus statement by the International Myeloma Working Group. Lancet Oncol **2017**;18:e206-e17
38. Hui S, Ghergurovich JM, Morscher RJ, Jang C, Teng X, Lu W*, et al.* Glucose feeds the TCA cycle via circulating lactate. Nature **2017**;551:115-8
39. Hensley CT, Faubert B, Yuan Q, Lev-Cohain N, Jin E, Kim J*, et al.* Metabolic Heterogeneity in Human Lung Tumors. Cell **2016**;164:681-94
40. Deaglio S, Morra M, Mallone R, Ausiello CM, Prager E, Garbarino G*, et al.* Human CD38 (ADP-ribosyl cyclase) is a counter-receptor of CD31, an Ig superfamily member. J Immunol **1998**;160:395-402
41. Ferrero E, Malavasi F. Human CD38, a leukocyte receptor and ectoenzyme, is a member of a novel eukaryotic gene family of nicotinamide adenine dinucleotide+-converting enzymes: extensive structural homology with the genes for murine bone marrow stromal cell antigen 1 and aplysian ADP-ribosyl cyclase. J Immunol **1997**;159:3858-65
42. Liu X, Grogan TR, Hieronymus H, Hashimoto T, Mottahedeh J, Cheng D*, et al.* Low CD38 Identifies Progenitor-like Inflammation-Associated Luminal Cells that Can Initiate Human Prostate Cancer and Predict Poor Outcome. Cell Rep **2016**;17:2596-606
43. Fernandez JE, Deaglio S, Donati D, Beusan IS, Corno F, Aranega A*, et al.* Analysis of the distribution of human CD38 and of its ligand CD31 in normal tissues. J Biol Regul Homeost Agents **1998**;12:81-91
44. Morandi F, Morandi B, Horenstein AL, Chillemi A, Quarona V, Zaccarello G*, et al.* A non-canonical adenosinergic pathway led by CD38 in human melanoma cells induces suppression of T cell proliferation. Oncotarget **2015**;6:25602-18
45. Lee CU, Song EK, Yoo CH, Kwak YK, Han MK. Lipopolysaccharide induces CD38 expression and solubilization in J774 macrophage cells. Mol Cells **2012**;34:573-6
46. Pepping JK, Vandanmagsar B, Fernandez-Kim SO, Zhang J, Mynatt RL, Bruce-Keller AJ. Myeloid-specific deletion of NOX2 prevents the metabolic and neurologic consequences of high fat diet. PLoS One **2017**;12:e0181500
47. Quarona V, Zaccarello G, Chillemi A, Brunetti E, Singh VK, Ferrero E*, et al.* CD38 and CD157: a long journey from activation markers to multifunctional molecules. Cytometry B Clin Cytom **2013**;84:207-17
48. Christen S, Lorendeau D, Schmieder R, Broekaert D, Metzger K, Veys K*, et al.* Breast Cancer-Derived Lung Metastases Show Increased Pyruvate Carboxylase-Dependent Anaplerosis. Cell Rep **2016**;17:837-48

MM#	Sex	Age	Isotype	% Plasmacytosis
#1	M	82	IgG	90
#2	F	76	Kappa LC	70
#3	F	79	IgA	90
#4	F	75	Lambda LC	65
#5	M	90	IgG	90
#6	M	96	IgG	25
#7	F	89	IgG	30
#8	M	62	IgG	65
#9	F	75	IgA	50
#10	M	73	Kappa LC	75
#11	M	78	IgG	90

Table 1. Patient information of primary MM samples used in this study.

Figure Legends

Figure 1. MM favours oxidative phosphorylation in the presence of the BMM. Primary MM cells were analysed using the Seahorse extracellular flux assay with Mito Stress kit. All Seahorse extracellular flux experiments were carried out in Seahorse conventional Mitostress base media containing 2.5/10mM Glucose, 2mM glutamine and 1mM pyruvate. (A) Oxygen consumption rate (OCR) of two primary MM cells and two MM cell lines are presented. (B) Basal mitochondrial respiration of MM cell lines (n=4) vs primary MM cells (n=4). (C) Basal glycolysis rates of MM cell lines (n=4) vs primary MM cells (n=4). (D-F) MM1S-luc cells were injected in NSG mice (n=6), 2 weeks after injection the MM cells were sorted from the mouse bone marrow. (D) Oxygen consumption rate (OCR) of MM1S cells grown in-vitro and MM1S cells isolated from mice. Basal mitochondrial respiration (E) and glycolysis rates (F) of MM1S cells grown in-vitro and MM1S cells isolated from mice. (G-I) MM cell lines were grown with and without BMSC for 72 hours, MM cells were then analysed by Seahorse. (G) Oxygen consumption rate (OCR) of MM1S cells grown with and without BMSC. Basal mitochondrial respiration (H) and glycolysis rates (I) of MM1S, U266 and RPMI grown with and without BMSC. (J) Growth capacity and ATP production was measured in MM1S, U266 and RPMI grown with and without BMSC for 72 hr. (K and L) MM cells were cultured in BMSC conditioned medium +/- 0.2µm filtration for 24 hours, followed by Seahorse extracellular flux analysis (K) or CellTitre-Glo ATP analysis. (M) BMSC were treated with 25µM rotenone or DMSO for 30 minutes before co-culture with MM cells. Mitochondrial respiration was measured in MM using the Seahorse extracellular flux assay. (N) The seahorse extracellular flux assay in (H) was repeated in 10mM glucose MitoStress conventional base medium.

Figure 2. Mitochondria are transferred from BMSC to MM cells in-vitro and in-vivo. Primary MM cells (n=10) (A) or MM cell lines (n=5) (B), were pre-stained with 200nM MitoTracker Green FM, were cultured for 24 hours on BMSC stained with MitoTracker Green FM. MitoTracker fluorescence was analysed in the MM cells by flow cytometry. (C) RPMI MM cell line was grown on rLV.EF1.mCherry BMSC, mCherry acquisition by MM cells was detected by fluorescent microscopy. (D) NSG mice were injected with either MM1S-luc cells or U266-Luc cells. 2 weeks post

engraftment MM cells were isolated from the BM and total DNA was extracted from the purified MM populations and analysed by PCR for murine and human specific mitochondrial and genomic DNA. PCR products were visualised by agarose gel electrophoresis. (E) Primary MM#1 was treated with 25 μM rotenone or DMSO for 15 minutes, then washed and cultured with or without BMSC. MM cells were then stained with 30 nM TMRM for 15 minutes before flow cytometry analysis. Representative flow cytometry plots are presented. (F) Primary MM and MM cell lines (n=5) were treated as in (E), TMRM ratio of rotenone/DMSO of MM cells grown with and without BMSC is presented. (G) and (H) Mitochondrial transfer levels were assessed, using MitoTracker Green, to primary MM cells (n=7) (G) or MM cell lines (n=4) (H) upon the addition of 10 nM Bortezomib. (I) Rho0 BMSC were generated from the BMSC cell line HS-5. MM primary cells were then grown on control BMSC or rho0 BMSC for 48 48 hours, MM cells were then analysed by Seahorse for oxygen consumption rate at basal and maximal conditions.

Figure 3. Mitochondrial transfer in MM is via TNTs. MM cell lines and BMSC were pre-stained with 200 nM MitoTracker green for 1 hour and then cultured together before 24-hour drug treatment, with 350 μM Cytochalasin B (A) and 50 μM Dansylcadavarine (B). Flow cytometry was used to detect MitoTracker green FM in the MM cells. (C) MM1S cells were stained with vybrant DiI for 1 h and washed 3 times in PBS. BMSC were stained with MitoTracker green FM for 1 h and washed 3 times in PBS. MM cells and BMSC were then co-cultured for 24 hours before fixation using paraformaldehyde. Cells were visualised by confocal microscopy. (D-E) MM1S cells lentivirally transduced with the rLV.EF1.AcGFP-Mem9 virus were cultured with BMSC stained with MitoTracker CMXRos for 24 hours before fixation with paraformaldehyde. Confocal microscopy imaging highlighted TNTs formed between the MM and BMSC. (F) U266 MM cells and BMSC were prepared and cultured as in (C). U266 MM cells were washed off prior to fixation. TAPs on BMSC were visualised by confocal microscopy and quantified on each confocal image obtained (n=5). (G) This was carried out also for MM cell lines MM1s, RPMI and H929.

Figure 4. CD38 inhibition prevents mitochondrial transfer and TNT formation. (A) Mitochondrial levels in primary MM cells (n=7) and MM cell lines (n=5) were

correlated to CD38 expression on these cells. Mitochondrial levels were achieved using the MitoTracker based assay, whilst CD38 expression was determined using flow cytometry. (B) Primary MM cells (n=8) and BMSC were pre-stained with 200 nM MitoTracker green for 1 hour and then cultured together before 24-hour treatment with a CD38 blocking antibody. Flow cytometry was used to detect MitoTracker green FM in the MM cells. (C) Four MM cell lines were transduced with a lentivirus targeted to CD38 or control for 72 hours. CD38 protein expression levels were analysed by flow cytometry. (D) The four MM cell lines transduced with a lentivirus targeted to CD38 or control were pre-stained, along with BMSC, with MitoTracker green for 1 hour and then cultured together for a further 24 hours before MitoTracker was assayed by flow cytometry. (E and F) Control KD and CD38 KD MM1S and U266 cells were co-cultured with BMSC for 24 hours. Cell viability and levels of apoptosis were assessed using CellTitre-Glo and Annexin V staining respectively. (G and H) U266, RPMI and H929 cells were treated with 1μM ATRA or DMSO overnight. CD38 expression was analysed in MM cells at RNA (G) and protein (H) levels, using qPCR and flow cytometry respectively. (I) Mitochondrial transfer levels from BMSC to MM cells was analysed using the MitoTracker green mitochondrial transfer assay, after treatment of MM cells with ATRA.

Figure 5. Tumor cell CD38 supports the formation of TNTs. (A) MM1S, U266, RPMI and H929 MM cell lines, transduced with a lentivirus targeted to CD38 or control, were stained with Vybrant DiI for 1 h and washed 3 times in PBS. BMSC were stained with MitoTracker green FM for 1 h and washed 3 times in PBS. MM cells and BMSC were then co-cultured for 24 hours, MM cell lines removed before fixation using paraformaldehyde. TAPs were visualised on BMSC by confocal microscopy. (B) TAPs formed by control KD and CD38 KD cells were quantified on BMSC using confocal images obtained (n=5). (C and D) MM1S and U266 MM cell lines were co-cultured with BMSC for 24 hours. Cells were removed and analysed for CD38 expression by flow cytometry. (E) The location of CD38 on BMSC, after TAP formation by MM1S cells, was determined by staining with a CD38 antibody (Alexa Fluor 647). TAPs and CD38 expression were visualised on BMSC by confocal microscopy.

Figure 6. Targeting CD38 in-vivo blocks mitochondrial transfer and improves animal survival. (A) Mice were imaged using bioluminescence weekly to monitor engraftment and disease progression in the animals injected with control and CD38 KD MM1S-luc cells. (B) The survival of NSG mice injected with either control KD or CD38 KD MM1S-luc cells. (C) Control KD and CD38 KD MM1S-luc cells were plated at a concentration of $100x10^3$ cells/ml. The growth capacity of both cell types was monitored over a 72hr period using trypan blue exclusion. (D) Mitochondrial levels were analysed in the purified control KD and CD38 KD MM cells, after isolation from recipient animals, by staining for 15 minutes in 200 mM MitoTracker Green and flow cytometry. (E) Mitochondrial levels in control KD and CD38 KD MM cells cultured in-vitro were analysed MitoTracker fluorescence. (F) CD38 KD and control KD MM1S cells were grown in-vitro with and without BMSC for 72 hr, prior to analysis by the Seahorse extracellular flux analyser with Mito Stress kit. (G) Oxygen consumption rate (OCR) of CD38 KD and control KD MM1S cultured with BMSC. Data represented as mean +/- standard deviation. (F) Basal mitochondrial respiration of CD38 KD and control KD MM1S cells grown with and without BMSC.

Figure 1

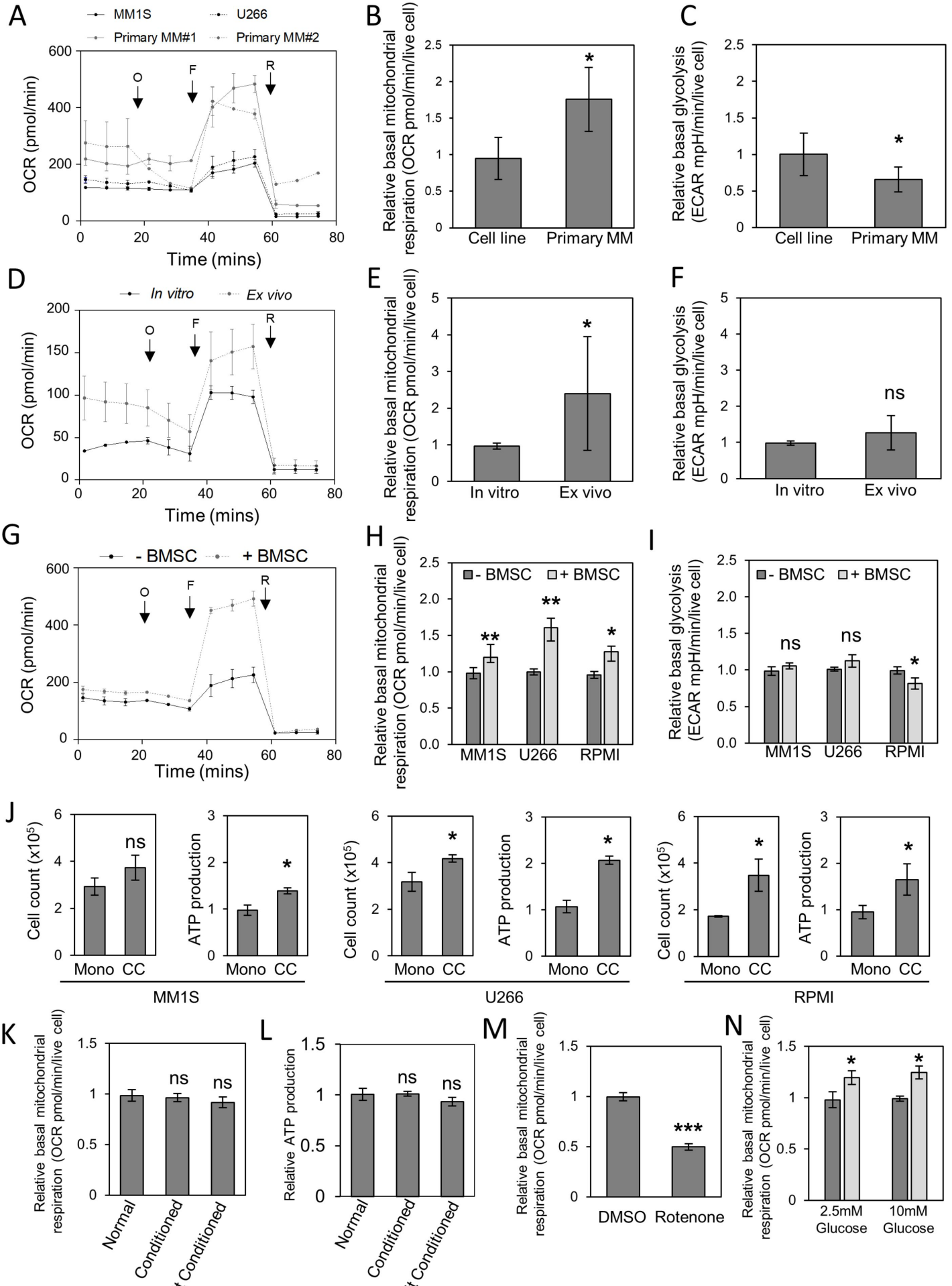

Figure 2

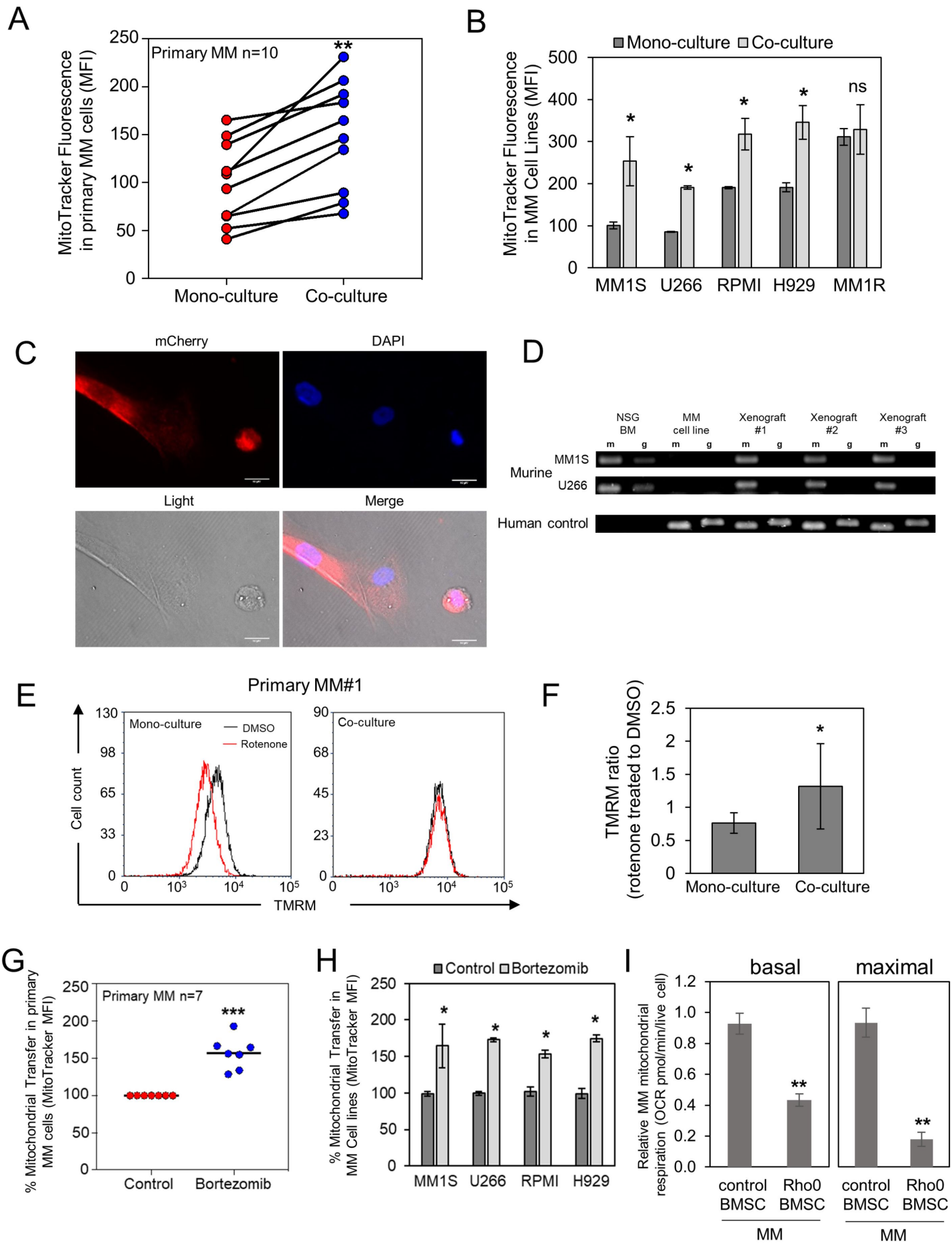

Figure 3

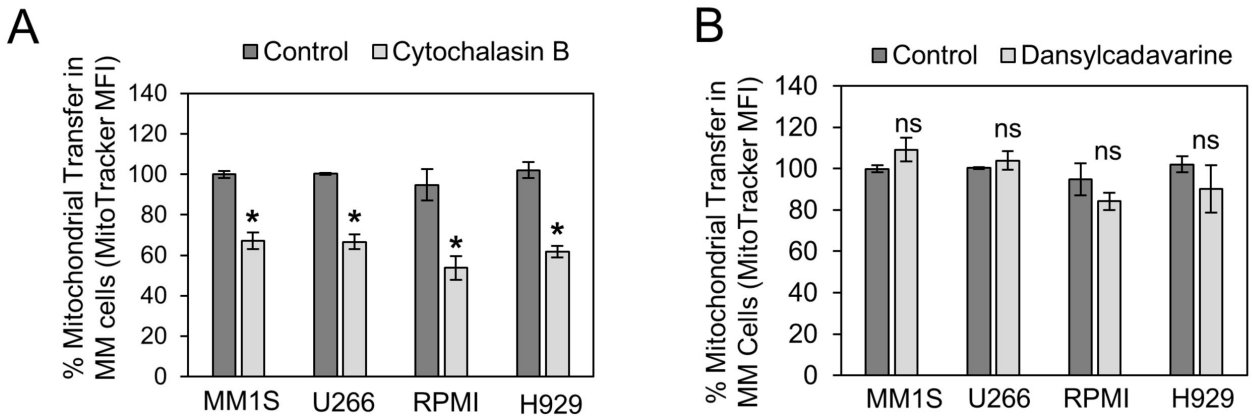

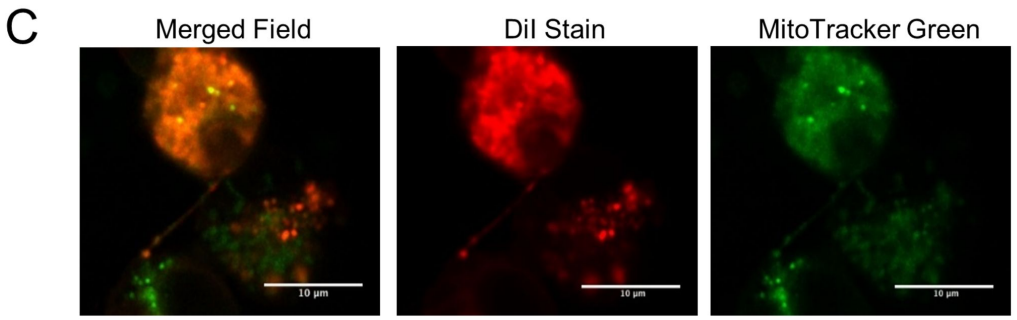

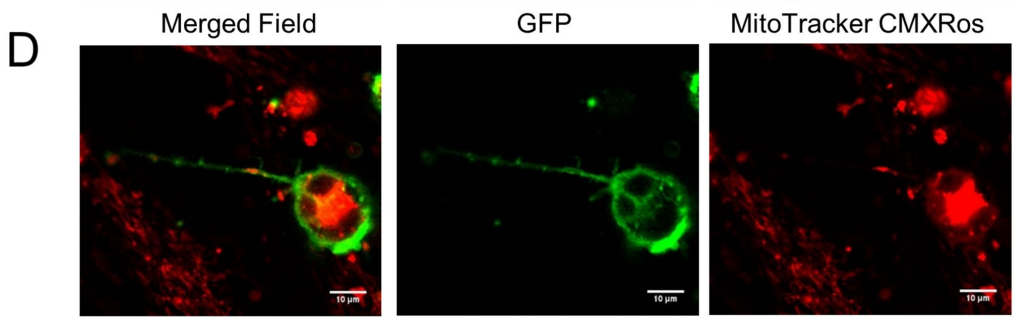

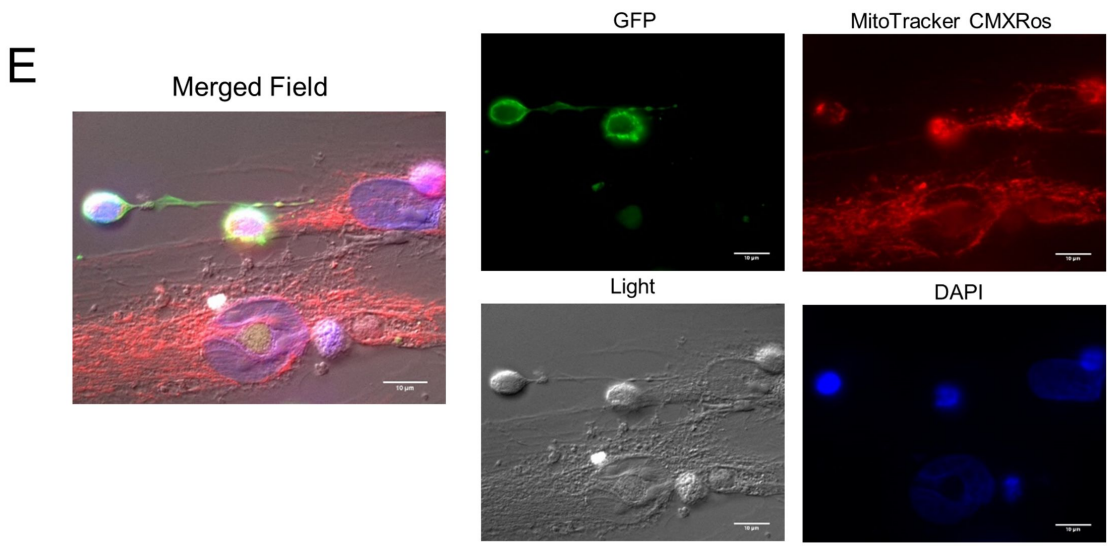

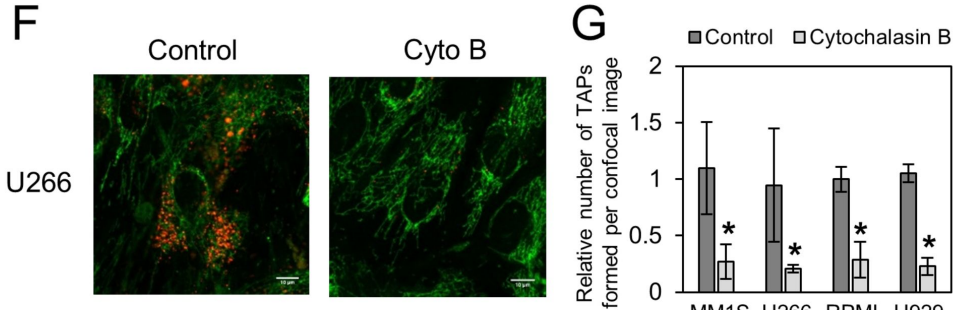

Figure 4

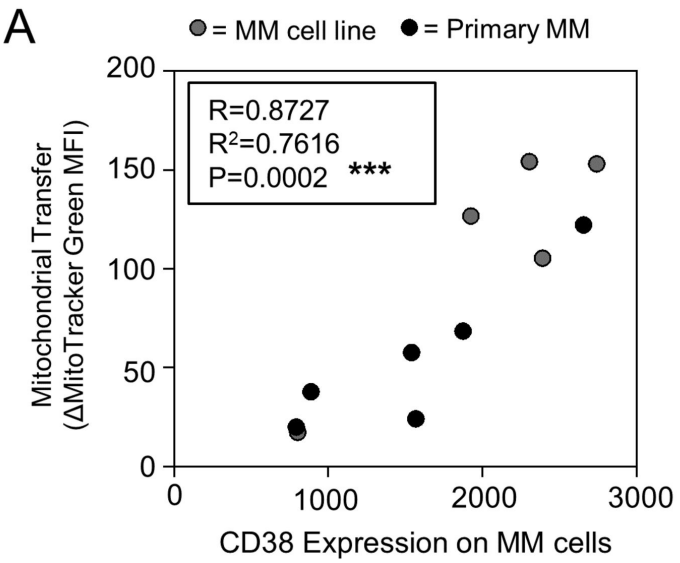

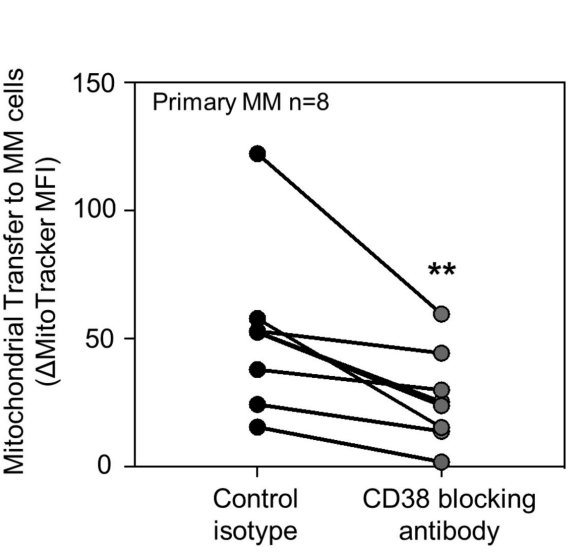

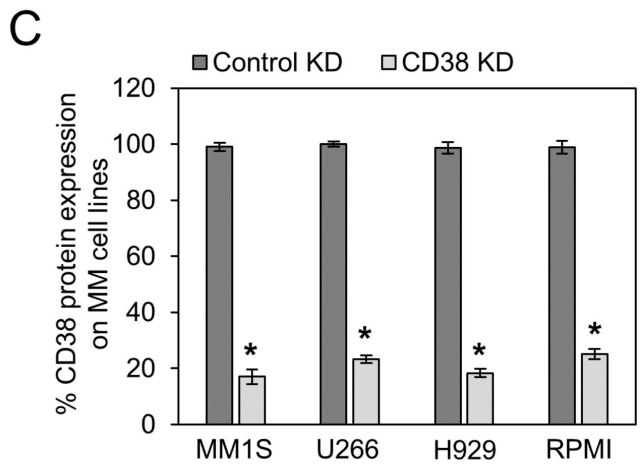

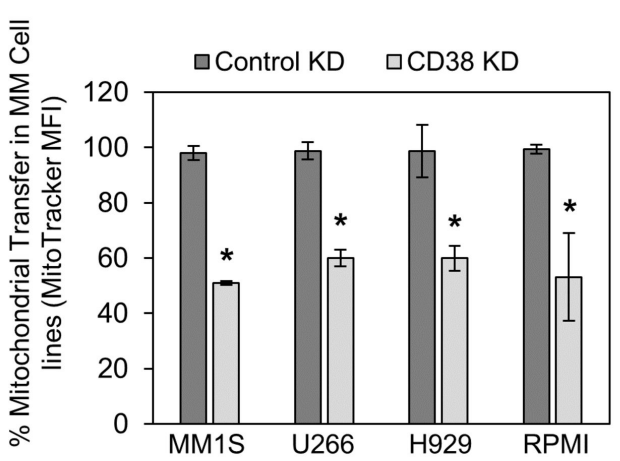

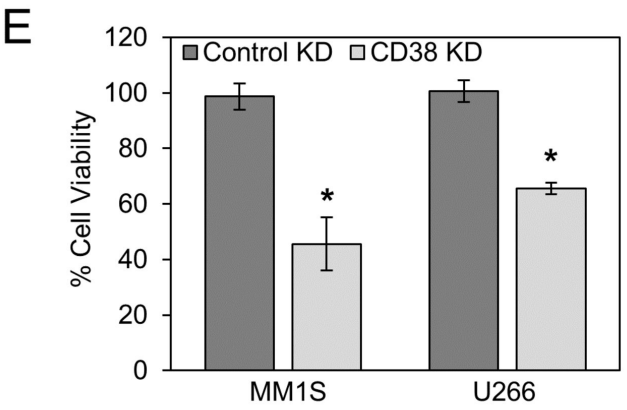

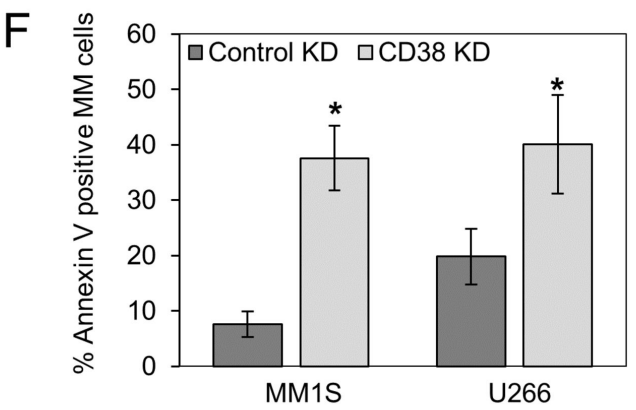

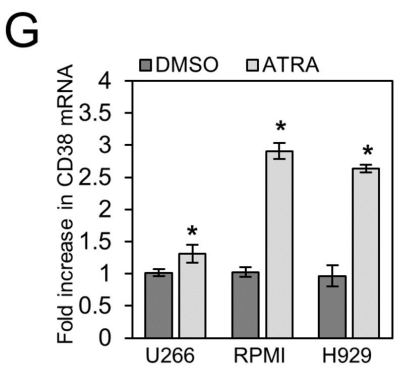

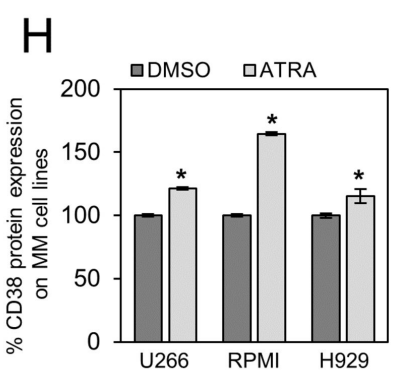

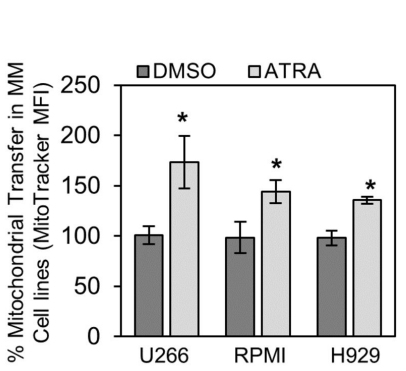

Figure 5

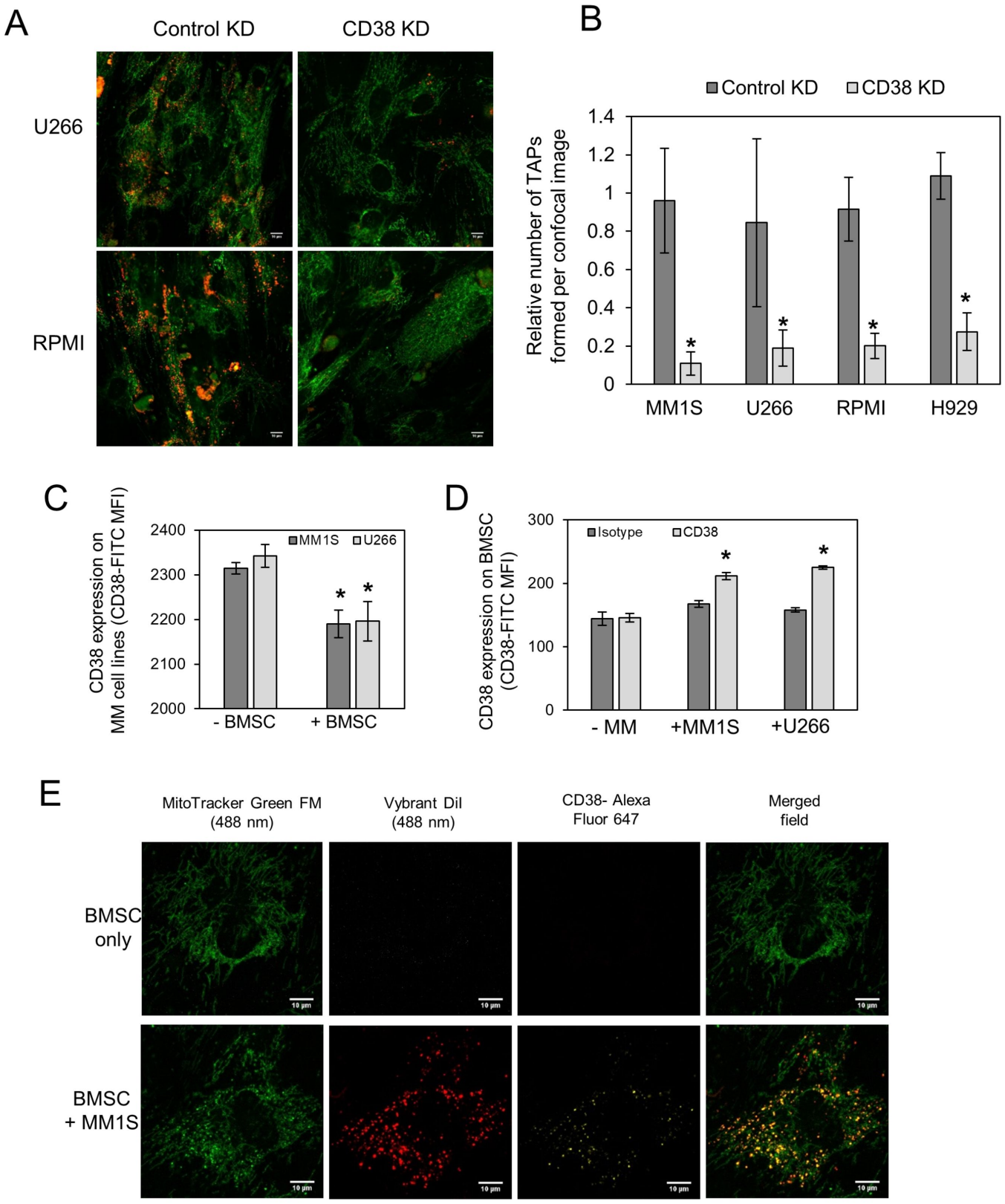

Figure 6

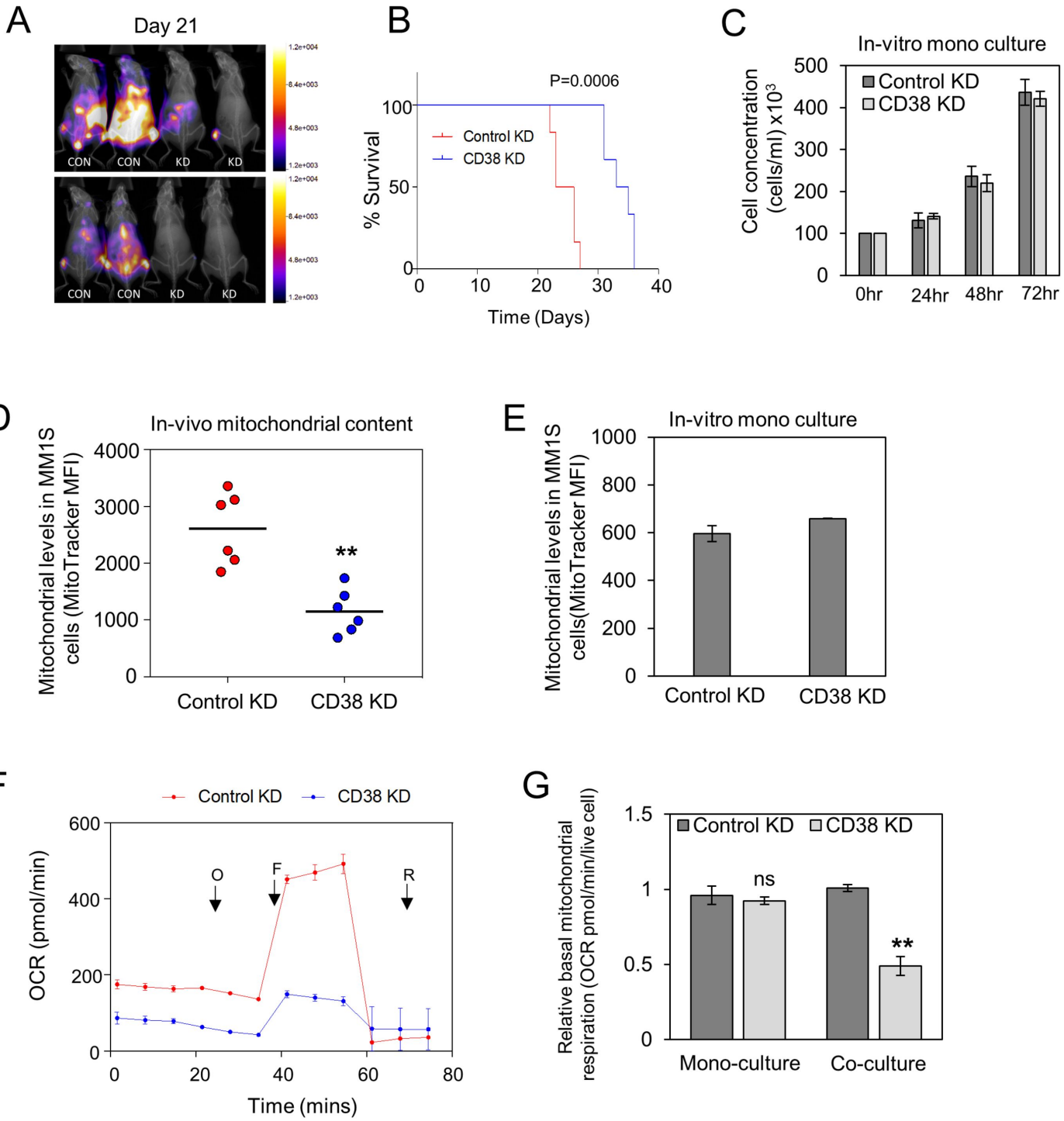

AACR American Association for Cancer Research

Cancer Research

The Journal of Cancer Research (1916–1930) | The American Journal of Cancer (1931–1940)

CD38-driven mitochondrial trafficking promotes bioenergetic plasticity in multiple myeloma

Christopher R. Marlein, Rachel E. Piddock, Jayna J. Mistry, et al.

Cancer Res Published OnlineFirst January 8, 2019.